

BEAM ACCELERATION WITH THE UPGRADED RIKEN HEAVY-ION LINAC

T. Nishi*, M. Fujimaki, N. Fukunishi, H. Imao, O. Kamigaito, T. Nagatomo,
N. Sakamoto, A. Uchiyama, T. Watanabe, Y. Watanabe, K. Yamada
RIKEN Nishina Center, Wako, Japan

Abstract

The performance of the RIKEN heavy-ion linac (RILAC) has been upgraded with a new electron cyclotron resonance ion source and superconducting linac booster (SRILAC). It is expected to have a major role in the synthesis of superheavy elements (SHEs), development of the technologies for production of medical radioisotopes, and as a powerful injector to the RI Beam Factory. Here, we report on the beam delivery for the SHE experiment that began in June 2020, particularly on the adjustment of the optics based on the measured phase ellipse.

INTRODUCTION

The RIKEN Nishina Center has been conducting experiments to search for new superheavy elements using RIKEN heavy-ion linac (RILAC) [1]. Recently, a new 28-GHz electron cyclotron resonance (ECR) ion source [2] and superconducting linear accelerator (SRILAC) [3] were constructed to increase the beam intensity and beam energy. The low-energy beam-transport (LEBT) system is equipped with slit triplets that control the beam emittance in the RILAC. The beam energy and beam positions are measured using eight sets of capacitive pickups called BEPM (beam energy position monitor) installed in the cold section of the SRILAC [4, 5].

In January 2020, we obtained the first beam from SRILAC. The Ar^{11+} with an intensity of $2 \mu\text{A}$ was accelerated up to 5 MeV/u [6]. From July 2020, we began to deliver the high-intensity V^{13+} beam with energy of 6 MeV/u to the GARIS-III [7] experiment. To transport the high-intensity heavy ion beam to the GARIS-III target with acceptable beam loss, we have established a method of measuring the phase ellipse and adjusting the optics based on the measured phase ellipse and optical simulation. This method enables us to optimize the optics flexibly according to the beam state, which varies depending on the ion source and slit conditions, as well as the experimental requirements.

HIGH ENERGY BEAM TRANSPORT LINE

The heavy ion beam, accelerated to approximately 6 MeV/u in the SRILAC, passes through a differential pumping system [8] and is then transported to GARIS-III through a beam transport called the high-energy beam transfer (HEBT) line (Fig. 1). The inner diameter of this beam transport is 62 mm, and its configuration is TQ - TQ - D - SQ - SQ - DQ (TQ = triplet quadrupole, D = dipole, SQ = singlet quadrupole, DQ = doublet quadrupole). D is a 90° bending

* takahiro.nishi@riken.jp

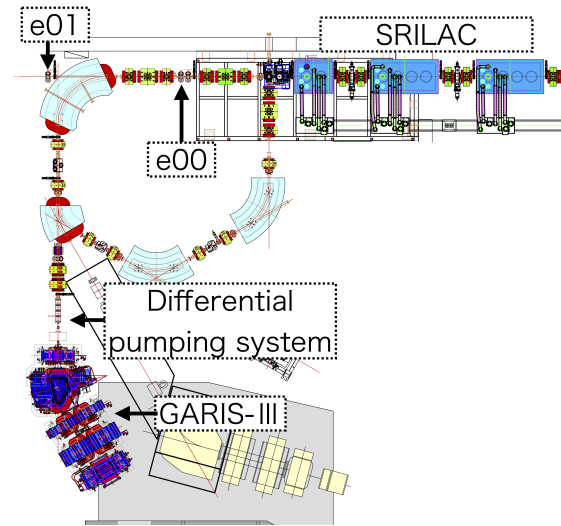


Figure 1: Top view of SRILAC, high-energy beam transfer line, and GARIS-III. A middle point denoted as e00 is considered the object point for optical calculation.

magnet with edges cut at 25° at both ends. Additionally, a bending magnet is placed between SQ and DQ, but it is not excited during the beam transport to GARIS-III. GARIS-III is filled with He gas at $\approx 70 \text{ Pa}$ during the experiment, while the vacuum of the HEBT line must be maintained at 10^{-5} – 10^{-6} Pa . Therefore, the inner diameter of the beam pipe immediately before the target is narrowed to $\phi 25$ -15 mm, and the gas is continuously evacuated by a vacuum pump. The requirements for the beam transport of the HEBT line are (A) a beam loss less than a few percent and (B) the adjustability of beam spot shape on the GARIS-III target depending on the experimental conditions. The first requirement is particularly important for maintaining for the radiation safety. Since the side wall of GARIS-III is relatively thin, it is necessary to measure and confirm the radiation while optimizing the beam transport. For the second requirement, a horizontally flatted ellipse is desired in the production run to prevent local depletion of the rotating target, while a large circle shape is desired in the calibration run. To satisfy these requirements, the beam envelope should be narrower immediately before the target, where the acceptance is relatively smaller and wider at the target.

PHASE ELLIPSE MEASUREMENT AND OPTICS TUNING

In the operations of the upgraded RILAC, the optical system was adjusted in two steps. First, phase ellipse of the beam at e00, defined as the object point in the optical

design, was measured using the wire scanner at e00 and e01 (Fig. 1). The phase ellipse at e00 was adjusted to be upright using a triplet quadrupole upstream of e00 based on optical calculation. Second, the optics from the object point to the target of GARIS-III experiment were tuned using optical simulation based on the adjusted phase ellipse at e00 and experimental requirement for beam spot shape. Details of these steps are described below.

(1) Phase Ellipse Measurement and Adjustment

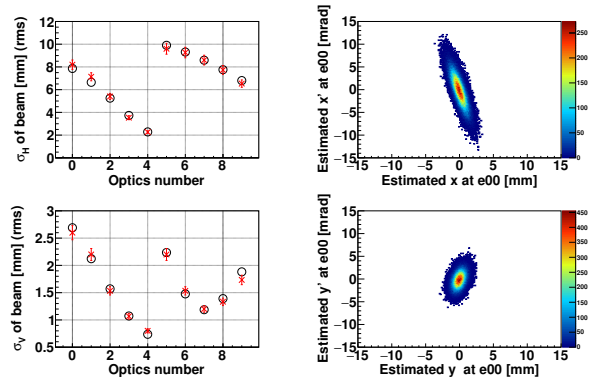
The phase ellipse at the object point was measured using wire scanners and triplet quadrupole magnets in the straight line from e00 to e01 (Fig. 1). The beam widths in horizontal and vertical directions were measured using 10 different settings of quadrupoles inbetween. The phase ellipse at e00 was estimated to reproduce the beam widths in all settings simultaneously. These 10 optical systems were selected to be sensitive to any type of phase ellipses using optical simulation.

The measured phase ellipse was adjusted to be upright using the triplet quadrupole magnets located upstream of e00. Based on the current magnetic field of these magnets and the measured phase ellipse, a new optics was calculated and adopted. Figure 2 shows an example of the estimated phase ellipse at e00 before and after the phase ellipse adjustment. These measurements were performed on an approximately 100 enA V^{13+} beam accelerated to 6 MeV/u. The graph on the left shows the beam widths (rms) measured at e01 for each optical setting, where the red crosses represent the measured values and the black circles represent the fitted results. The contour plots on the right are the phase ellipses at e00 estimated from the fitted results. Here, the phase ellipse was assumed to have a two-dimensional normal distribution. As shown in the figures, the phase ellipse was tilted before adjustment and became upright after the adjustment as calculated. The measured emittances in these measurements were $\epsilon_h = 5.73$ and $\epsilon_v = 3.30$ before the adjustment and $\epsilon_h = 5.67$ and $\epsilon_v = 3.27$ after the adjustment (both corresponding to 4 rms, unit is [π mm mrad]), which were in good agreement with each other.

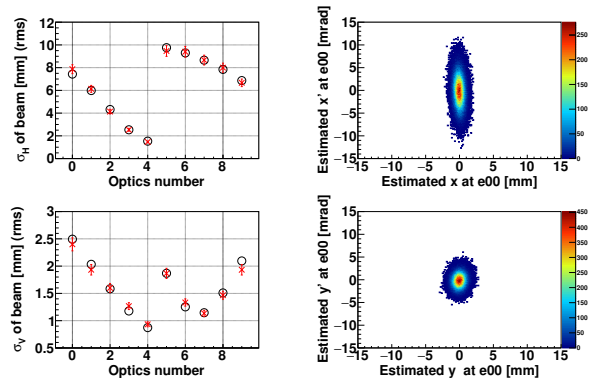
Some of the emittance values measured from January 2020 to July 2021 are summarized in Table 1. The emittance values measured at e00 were approximately 2 to 7 [π mm mrad] for both ϵ_h and ϵ_v . As shown in the table, the values of emittance varied in each measurement. Therefore, it is important to measure the phase ellipse at each operation of the ion source and accelerator and to optimize the optics to the phase ellipse as in the method used in this study.

The data in 2nd and 3rd rows or 5th and 6th rows correspond to the beam emittance in the series operations before and after acceleration by SRILAC, respectively. These data indicate that the beam emittance reduced by the SRILAC acceleration to almost the expected values.

" ϵ at upstream" in Table 1 is the emittance measured at the pepperpot placed upstream of the radio frequency quadrupole (RFQ). Considering the energy of the particles here (≈ 3 keV/u), the emittance downstream increased by a



(a) Measured beam widths and estimated phase ellipse before adjustment.



(b) Measured beam widths and estimated phase ellipse after adjustment.

Figure 2: Data of emittance measurement before (a) / after (b) adjustment of phase ellipse at an object point e00.

factor of approximately 1.5 to 6 of the expected value. The detailed cause of this results is currently under analysis.

The measurement of the phase ellipse and upright adjustment of the phase ellipse were almost automated except for the data acquisition by the wire scanners. The phase ellipse measurement required approximately 30 min and the entire procedure to measure and adjust the phase ellipse required 1 hour.

(2) Optics Tuning to a Target for GARIS-III

After confirming that the phase ellipse was upright at e00, we optimized the optical system from e00 to the GARIS-III target based on the measured phase ellipse. In the basic optical system, the image magnification from e00 to GARIS-III was set to 1.0 in both horizontal and vertical directions. The optics was adjusted to satisfy the required spot shape and acceptable beam loss simultaneously using the optical simulation code GICOSY [9] and Monte Carlo simulation MOCADI [10]. Finally, the optical system was optimized by fine-tuning the steerer and the magnetic field of each magnet based on the viewer on the target, baffles located upstream of the target, and beam current measured using a Faraday cup.

Table 1: Measured Emittance of Heavy-Ion Beams Accelerated by SRILAC

| Ion | Energy [MeV/u] | ϵ_h at e00 [π mm mrad] | ϵ_v at e00 [π mm mrad] | ϵ_h at upstream [π mm mrad] | ϵ_v at upstream [π mm mrad] |
|-------------------|----------------|--------------------------------------|--------------------------------------|---|---|
| Ar ¹³⁺ | 4 | 3.6 | 2.7 | — | — |
| Ar ¹³⁺ | 4 | 5.5 | 2.7 | — | — |
| Ar ¹³⁺ | 6 | 3.9 | 2.3 | — | — |
| Ar ¹³⁺ | 6 | 4.0 | 6.0 | 34.2 | 41.2 |
| Ar ¹³⁺ | 4 | 4.7 | 6.8 | 92.9 | 83.2 |
| Ar ¹³⁺ | 6 | 3.6 | 4.3 | — | — |
| Ar ¹³⁺ | 6 | 3.2 | 3.2 | 99.3 | 63.5 |
| Ar ¹¹⁺ | 5 | 3.1 | 6.5 | — | — |
| Ar ¹¹⁺ | 5 | 2.2 | 1.6 | — | — |
| V ¹³⁺ | 6 | 5.9 | 4.5 | 84.1 | 66.4 |
| V ¹³⁺ | 6 | 5.7 | 3.3 | — | — |

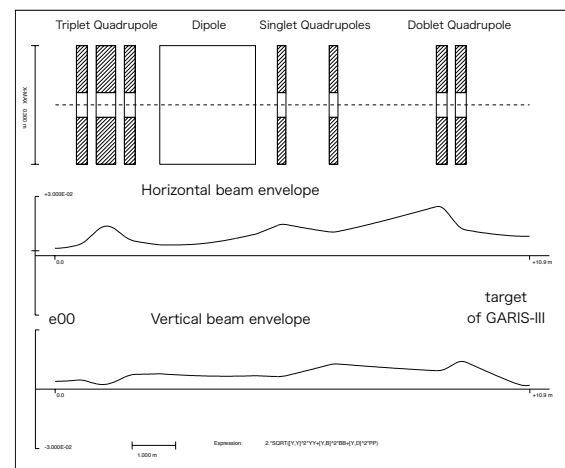
Figure 3 (a) depicts to the optics used for the beam transport with the phase ellipse in Fig. 2 (b). The top row of the figure shows the optical elements after e00 of the HEBT line, and the second and third rows show the beam envelopes in the horizontal and vertical directions, respectively. These images were created using GICOSY. The image magnification was set to 2.5 in the horizontal direction and 0.5 in the vertical direction to realize a horizontal elliptical spot. Figure 3 (b) shows a charge-coupled device (CCD) camera image of the beam spot on the target after the adjustment of the steerer, etc. Although the emittance was almost twice as large in the vertical direction, the beam spot was wide in the horizontal direction as required by adjusting the optical system. In this transportation, the beam loss was suppressed to a few percent. The outdoor radiation level was measured and confirmed to be within the acceptable level.

REAL-TIME EMITTANCE MEASUREMENT USING THE BEPM

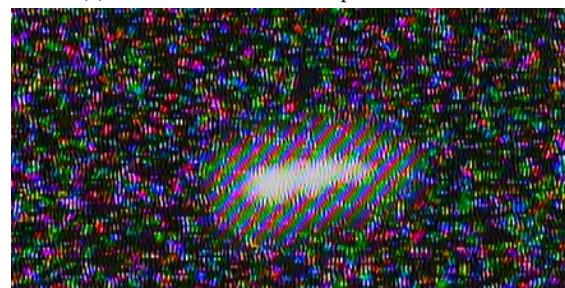
While beam emittance measurement with wire scanners in SRILAC is effective as described above, the method requires the beam current to be reduced to less than 100 enA and the magnetic currents to be changed. To realize more effective optimization of optics in the HEBT line in long-term operations, we require real-time emittance measurement.

We are developing a new method of measuring beam emittance using non-destructive diagnostics: beam energy position monitor (BEPM). Eight BEPMs are installed in-between quadrupole magnets in the SRILAC. The BEPM consists of four electrodes and measures the beam position and time of flight in-between using the induced voltage on the electrodes. Now, we are attempting to utilize the detectors to estimate the beam phase ellipse.

The asymmetry of signal strength of four electrodes reflect the flatness of a beam ellipse [11, 12]. The standard deviation of horizontal and vertical beam position distribution σ_x and



(a) Calculated beam envelope in HEBT line.



(b) Beam spot on target.

Figure 3: (a) Top figure represents optical elements. The middle and bottom figures show the beam envelope in horizontal and vertical directions, respectively. (b) Beam spot captured using a CCD camera on a viewer at the GARIS-III target. The beam spot was horizontally flatted ellipse as expected.

σ_y can be related to the BEPM signals as

$$Q \equiv \sigma_x^2 - \sigma_y^2 = k_q \frac{V_L + V_R - V_U - V_D}{V_L + V_R + V_U + V_D} - \langle x \rangle^2 + \langle y \rangle^2, \quad (1)$$

where V_L , V_R , V_U , and V_D are the induced voltages of left, right, up, and down electrodes, respectively, and k_q is a con-

stant number measured previously. This value of Q is measured in each BEPM position, and it can be also calculated using components of sigma matrix and transfer matrices as

$$\begin{pmatrix} Q_1 \\ Q_2 \\ \vdots \\ Q_8 \end{pmatrix} = (\mathbf{H}, \mathbf{V}) \begin{pmatrix} \sigma_{xx}(0) \\ \sigma_{xa}(0) \\ \sigma_{aa}(0) \\ \sigma_{yy}(0) \\ \sigma_{yb}(0) \\ \sigma_{bb}(0) \end{pmatrix}, \quad (2)$$

where

$$\mathbf{H} \equiv \begin{pmatrix} (M_{11}^{01})^2, 2M_{11}^{01}M_{12}^{01}, (M_{12}^{01})^2 \\ \vdots \\ (M_{11}^{08})^2, 2M_{11}^{08}M_{12}^{08}, (M_{12}^{08})^2 \\ \vdots \\ -(M_{33}^{01})^2, -2M_{33}^{01}M_{34}^{01}, -(M_{34}^{01})^2 \\ \vdots \\ -(M_{33}^{08})^2, -2M_{33}^{08}M_{34}^{08}, -(M_{34}^{08})^2 \end{pmatrix},$$

$$\mathbf{V} \equiv \begin{pmatrix} \vdots \\ \vdots \end{pmatrix}.$$

In these equations, $\sigma(0)$ indicates the elements of the sigma matrix of the beam at the upstream position denoted as 0, and M_{ij}^{0n} is the (i, j) -th element of transfer matrix from position 0 to the position of the n -th BEPM.

Figure 4 shows Q_8 measured using the most downstream BEPM and the estimated Q_8 , which is calculated based on the calculated transfer matrices and sigma matrix obtained using wire scanner measurements. As shown in the figure, the two values have a clear positive correlation. We will investigate the origin of the offset and attempt to reconstruct beam emittance by combining $Q_1 - Q_8$.

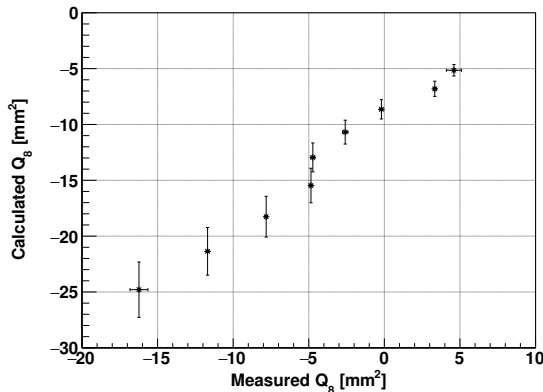


Figure 4: Comparison of the Q_8 measured using the most downstream BEPM and the estimated Q_8 , which is calculated based on the calculated transfer matrices and sigma matrix obtained using wire scanner measurements. The sigma matrix at position 0 is calculated with the phase ellipse at e00 and transfer matrix in between.

CONCLUSION

The performance of the RIKEN heavy-ion linac (RILAC) has been upgraded with a new ECR ion source and superconducting linac booster (SRILAC). We obtained the first beam in January 2020 and began to supply the V^{13+} beam to the experiment for the synthesis of super-heavy elements. In

the operation, we established the beam transport adjustment method and realized small beam loss and required beam spot shape simultaneously using wire scanners and simulation code. A new method to estimate the phase ellipse with non-destructive detector BEPMs is under development for the real-time measurement and optimization of the beam transport.

REFERENCES

- [1] K. Morita *et al.*, “New result in the production and decay of an isotope, $^{278}113$, of the 113th element”, *J. Phys. Soc. Jpn.*, vol. 81, p. 103201, 2012. doi:10.1143/JPSJ.81.103201
- [2] T. Nagatomo *et al.*, “High intensity vanadium beam for synthesis of new superheavy elements with well-controlled emittance by using slit triplet”, *Rev. Sci. Instrum.*, vol. 91, p. 023318, 2020. doi:10.1063/1.5130431
- [3] N. Sakamoto *et al.*, “Development of Superconducting Quarter-Wave Resonator and Cryomodule for Low-Beta Ion Accelerators at RIKEN Radioactive Isotope Beam Factory”, in *Proc. SRF2019*, Dresden, Germany, 2019, pp. 750–757. doi:10.18429/JACoW-SRF2019-WETEB1
- [4] T. Watanabe *et al.*, “Calibration for Beam Energy Position Monitor System for Riken Superconducting Acceleration Cavity”, in *Proc. IBIC2019*, Malmö, Sweden, 2019, pp. 526-529. doi:10.18429/JACoW-IBIC2019-WEPP007
- [5] T. Watanabe *et al.*, “Commissioning of the beam energy position monitoring system for the superconducting RIKEN eavy-ion linac”, in *Proc. IBIC2020*, Santos, Brazil, pp. 295-302. doi:10.18429/JACoW-IBIC2020-FRA004
- [6] K. Yamada *et al.*, “Construction of Superconducting Linac Booster for Heavy-Ion Linac at RIKEN Nishina Center”, in *Proc. SRF2019*, Dresden, Germany, 2019, pp. 502-507. doi:10.18429/JACoW-SRF2019-TUP037
- [7] H. Haba and for RIKEN SHE Collaboration, “Present Status and Perspectives of SHE Researches at RIKEN”, in *Proc. EXON-2018*, Petrozavodsk, Russia, 2019, 192-199. doi:10.1142/9789811209451_0027
- [8] H. Imao *et al.*, “Non-Evaporative Getter-Based Differential Pumping System for SRILAC at RIBF”, in *Proc. SRF2019*, Dresden, Germany, 2019, p. 419–423. doi:10.18429/JACoW-SRF2019-TUP013
- [9] “GICOSY” on web page: <https://web-docs.gsi.de/~weick/gicosy/>
- [10] N. Iwasa, H. Geissel, G. Münzenberg, C. Scheidenberger, T. Schwab, and H. Wollnik, “MOCADI, a universal Monte Carlo code for the transport of heavy ions through matter within ion-optical systems”, *Nucl. Instrum. Methods Phys. Res., Sect. B*, vol. 126, pp. 284-289, 1997. doi:10.1016/S0168-583X(97)01097-5
- [11] R. H. Miller, J. E. Clendenin, M. B. James, and J. C. Shepard, “Nonintercepting emittance monitor”, in *Proc. HEAC’83*, Fermilab, IL, USA, 1983, pp. 602-605. <http://slac.stanford.edu/pubs/slacpubs/3000/slac-pub-3186.pdf>
- [12] T. Suwada, “Multipole Analysis of Electromagnetic Field Generated by Single-Bunch Electron Beams”, *Jpn. J. Appl. Phys.*, vol. 40, pp. 890-897, Jan. 2001.